Published in final edited form as:
Anal Chem. 2010 September 1; 82(17): 7068–7072. doi:10.1021/ac101377a.

Redox-Magnetohydrodynamic Microfluidics Without Channels and Compatible with Electrochemical Detection Under Immunoassay Conditions

Melissa C. Weston, **Christena K. Nash**, and **Ingrid Fritsch***
Department of Chemistry and Biochemistry, University of Arkansas, Fayetteville, AR 72701

Abstract

A unique capability of redox-magnetohydrodynamics (redox-MHD) for handling liquids on a small scale was demonstrated. A 1.2-μL solution plug was pumped from an injection site to a detector without the need for a channel to direct the flow. The redox pumping species did not interfere with enzymatic activity in a solution compatible with enzyme-linked immunoassays. Alkaline phosphatase (AP), a common enzyme label, converted *p*-aminophenyl phosphate (PAPP) to *p*-aminophenol (PAP_R) in the presence of 2.5 mM $Ru(NH_3)_6Cl_2$ and 2.5 mM $Ru(NH_3)_6\ Cl_3$, in 0.1 M Tris buffer (pH=9). A solution plug containing PAPP (no AP) was pumped through the surrounding solution containing AP (no PAPP), and the enzymatically-generated PAP_R was easily detected and distinguishable electrochemically from the pumping species with square wave voltammetry down to 0.1 mM concentrations. The test device consisted of a silicon chip containing individually-addressable microband electrodes, placed on a 0.5-T NdFeB permanent magnet with the field oriented perpendicular to the chip. A 8.0-mm wide × 15.5-mm long × 1.5-mm high volume of solution was contained by a poly(dimethylsiloxane) gasket and capped with a glass slide. A steady-state fluid velocity of ~30 μm/s was generated in a reinforcing flow configuration between oppositely polarized sets of pumping electrodes with ~2.1 μA.

Introduction

There is great interest in developing lab-on-a-chip devices that provide advantages over traditional laboratory analysis including low sample consumption and waste generation, faster analysis times, low fabrication costs, and portability.1 These systems can be employed in applications such as environmental monitoring, separations, and bio-detection. The most common microfluidic technique presently of interest for development of these devices is electrokinetic pumping. Electrokinetic pumping, however, requires high voltages (~100 V) that cause bubble formation from electrolysis of water2, 3 and is highly dependent on the physicochemical properties of the walls and thus flow rates change with solution composition and over time.4 Redox magnetohydrodynamics (redox-MHD) is an alternative approach to microfluidics and offers advantages such as low voltages, easy bi-directional pumping, simplicity of fabrication (in part, due to the variety of substrates suitable for device fabrication which do not affect redox-MHD pumping), and compatibility with and wettability by a variety

*To whom correspondence should be addressed. Tel: (479) 575-6499, Fax: (479) 575-4049, ifritsch@uark.edu.

Supporting Information Available

PAPP synthesis, brief descriptions regarding selection of experimental setup, including a figure of the setup, and pumping species, figures and a brief discussion of limits of detection of PAP_R, in and out of the presence of the pumping species, a quantitative discussion and figure involving introduction and removal of PAP_R from simultaneous pumping and detection at the microband arrays, and a description of the effect of an active detecting electrode between pumping electrodes on redox-MHD induced convection, including figures showing the effect, are included. This material is available free of charge via the Internet at http://pubs.acs.org.

of different solvents. 5-8 The only compositional requirement for device materials that is unique to a redox MHD pumping involves providing ion flux, which in our case is accomplished by the presence of electrodes.

In redox-MHD, the oxidation or reduction of an added electroactive species generates an ion flux, **j** (coulomb / (second square meter)), in the presence of a magnetic field, **B** (tesla), to produce a magnetohydrodynamic force, $\mathbf{F_B}$ (newton / cubic meter), whose magnitude and direction are governed by the cross product relationship, $\mathbf{F_B} = \mathbf{j} \times \mathbf{B}$, following the right hand rule. Redox-MHD offers a significant improvement over traditional MHD where large voltages are applied at electrodes in solutions containing supporting electrolyte alone to achieve desired fluid flow.9-15 However, in redox-MHD, the ion flux is controlled with redox chemistry that can be turned on and off at electrodes at strategic locations at low voltages (<1 V) and thus avoids bubble generation and electrode degradation. A shortcoming of redox-MHD that has been reported previously6, 8, 16 is the need for a high concentration (100s of mM) of redox species to provide a large enough current (and ion flux) so that a sufficient MHD force can be generated with the low magnetic fields of permanent magnets that are suitable for hand-held devices. High concentrations of redox molecules could cause interferences in detection methods through chemical or electron transfer reactions with the analyte of interest.

We have previously demonstrated redox-MHD for the enhancement of anodic stripping voltammetry.16-18 In those studies, the same electrode was used for both convective and detection functions. It is an example of how MHD can “grab” a fluid element and move it without requiring channel sidewalls for guidance. However, the high concentration of redox species used for convection in the deposition step needs to be rinsed away before the detection (stripping) step to avoid a high background signal. Also, millimeter-sized electrodes were needed to achieve a large enough **j** and therefore large $\mathbf{F_B}$ to cause sufficient flow to increase analyte delivery to the electrode surface and significantly enhance the signal two to three fold. To use redox-MHD to enhance convection at microelectrodes in low B fields, as might be of interest in a microfluidic device, it would be more efficient to separate the pumping (or stirring) function (taking place at larger electrodes, 100s μm to several mm) from the detecting function (taking place at smaller electrodes, ≤100 μm). This would offer the advantage of a flow-through system, capable of introducing sample and rinsing solutions across a surface in an automated fashion. We have also just recently determined that it is possible to observe MHD-convection in low concentrations of redox species (10 mM)[19] indicating that rinsing away the pumping species might not be necessary. Given these new developments, the goal of the work herein is to ascertain the suitability of redox-MHD microfluidics under conditions that are directly relevant to a lab-on-a-chip application, specifically enzyme-linked immunoassays with electrochemical detection.

Heterogeneous immunoassays have high specificity and have been built on multiple substrates including glass, silicon, polymers, and gold, all of which can be readily integrated into microfluidic systems.[20-23] Immunoassays are often limited by mass transfer, driven by diffusion, rather than binding kinetics to capture antigens and secondary antibodies and to generate detectable enzymatic products. This results in longer incubation times because of the small diffusion coefficients associated with large biological species. [24] Stirring, therefore, helps to increase the flux of the antigen and further decrease incubation times. Because of MHD’s unique abilities to direct, mix, and position fluids, all on a single device, redox-MHD-induced convection could serve as a method to introduce and replace solutions containing immunoassay components and wash buffers in addition to mixing these components on-chip to decrease incubation times.

In the work described here, we report the use of redox-MHD induced convection as an effective way to transport components of an immunoassay while detecting an electrochemically active

species, simultaneously. The redox MHD-induced convection is achieved by application of a low voltage (−0.25 V vs. Au quasi-reference) to a set of electrodes in a solution containing the pumping redox couple of $Ru(NH_3)_6^{2+/3+}$ at low concentrations in Tris buffer in the presence of a magnetic field (from a small, NdFeB permanent magnet). *p*-Aminophenol (PAP_R), which is the product of the reaction of *p*-aminophenylphosphate (PAPP) with the enzyme alkaline phosphatase (AP) commonly used in electrochemically based, heterogeneous enzyme-linked immunoassays,[25, 26] is directed by redox-MHD flow, with pumping electrodes, to a separate detecting electrode where square wave voltammetry (SWV) is performed for detection of PAP_R in the presence of the pumping species. The Tris buffer allows AP to exhibit excellent enzyme efficiency and PAPP to show good stability.[27]

Experimental

Chemicals and Materials

All chemicals were reagent grade and used as received. Aqueous solutions were prepared with high purity deionized water from Ricca Chemical Co. (Arlington, TX). AP from bovine intestinal mucosa in lyophilized powder form, *p*-aminophenol hydrochloride, palladium (10 wt% on activated carbon), magnesium chloride hexahydrate, and 0.02% (w/v) sodium azide were obtained from Sigma (St. Louis, MO). Polystyrene latex microspheres (10 μm diameter, 2.5 wt% dispersion in water), 4-nitrophenyl phosphate disodium salt hexahydrate, and ruthenium (II) hexaammine chloride were obtained from Alfa Aesar (Ward Hill, MA). The as-received ruthenium (II) hexaammine chloride contained the oxidized form, ruthenium (III) hexaammine chloride, as well. Solutions prepared from this solid comprised of approximately a 1:1 mole ratio of the two forms as determined by cyclic voltammetry at a microband electrode. Tris(hydoxymethyl)aminomethane was acquired from J. T. Baker. Pieces cut from a gold coin (Canadian Maple Leaf, 99.99%) placed in a molybdenum boat (Kurt J. Lesker Co., Pittsburgh, PA) and a chromium-plated tungsten rod (Kurt J. Lesker Company, Clairton, PA) served as Au and Cr sources for metal deposition, respectively. Silicon wafers (125-mm diameter, 600-650-μm thickness, and (100) orientation) with 2-μm, thermally-grown SiO_2, purchased from Silicon Quest International, were used as substrates for microband array fabrication. Benzocyclobutene, BCB (Cyclotene 4024-40) was obtained from Dow Chemical Company. Electrical connection of the potentiostat to on-chip contact pads was made using an edge connector (solder contact, 20/40 position, 0.05 in. pitch) from Sullins Electronics Corp. (San Marcos, CA). Ultra high purity compressed argon gas was obtained from AirGas, Inc. (Radnor, PA). The *p*-aminophenyl phosphate (PAPP) was synthesized as previously described,[28] and elaborated upon in the Supporting Information.

Buffer Solution

The 0.1 M Tris buffer solution was prepared with 0.10 M tris-hydroxymethyl)aminomethane, 1 mM magnesium chloride, and 0.02% (w/v) sodium azide at pH 9.0 (adjusted with 6 M HCl or 6 M NaOH). All solutions used were made from 0.1 M Tris buffer (pH 9.0) that was purged for at least 20 min before use and all solutions were kept under Ar between runs to minimize oxidation of $Ru(NH_3)_6^{2+}$ and PAP_R.

Microelectrode array chips

Detailed fabrication and characterization of microelectrode array chips is described elsewhere.[19] The 1 in. × 1 in. chips contained 16 individually-addressable Au microband electrodes (each was 2 mm long and 92 μm wide, and separated from adjacent bands by 107 μm gaps). A single electrode in the middle of the array, electrochemically oxidized (after masking off part with tape) to shorten it to be 1 mm long, served as the detecting electrode. Each chip also contained two on-chip Au quasi-reference electrodes (6 mm × 0.5 mm).

Electrochemical Control

A CHI 760B bipotentiostat (CH Instruments, Austin, TX) was used for chronoamperometry (CA) and square wave voltammetry in a three-electrode configuration. The detecting electrode was connected to working lead "one" from the bipotentiostat. Five microbands that were shorted together to form one set of pumping electrodes were attached to working lead "two". Six shorted microbands on the other side of the detecting electrode and 1100 μm away from the first set of pumping electrodes formed the second set of pumping electrodes at an opposite bias and were connected to the auxiliary lead. The distant on-chip quasi-reference electrodes were shorted together (2.0 mm^2 total active area).

Experimental Setup

The general experimental setup (see Figure S-1(a) in Supporting Information) and visualization of redox-MHD flow using microbeads were reported previously.[19] A poly(dimethylsiloxane), or PDMS, gasket (1500-μm thick with a rectangular cutout of 8.0 mm × 15.5 mm) was placed on top of the array chip and defined the height of the cell. The walls lining the cutout of the PDMS gasket were far enough from the pumping electrodes such that they did not define a "channel" but rather served to contain the solution. Thus, lateral movement of the solution plug was guided by the MHD force, instead of channel sidewalls. Two, 1-mm diameter holes were drilled through a glass microscope slide (25 mm × 12 mm) to form "ports" and allowed for solution introduction and removal. The glass slide was then taped (with single-sided invisible tape (Staples®, Framingham, MA) to the PDMS-array chip assembly to seal and hold the device together to ensure that the solution would not leak out (see Figure S-1a in Supporting Information). The volume of the solution plug was large enough so that the array chip, the floor of the device, and the glass slide, the lid of the device, prevented the plug's movement in the vertical dimension. The MHD force then directed the plug's movement laterally in only two-dimensions. This assembly was placed on top of one of the flat sides of a NdFeB cylindrical permanent magnet (a rod having dimensions of 1 in. diameter x 1 in. long, Amazing Magnets®, Irvine, CA), so that the microband array (having overall dimensions of ~3.1 mm × 2 mm for the set of 16 electrodes) was centered in the middle of the much larger circularly-shaped plane of the magnet. A dc magnetometer, AlfaLab, Inc., measured 0.5 T at the array.

The cell was filled with 250 μL of supporting electrolyte (0.1 M Tris buffer) containing a 1:1 mole ratio of oxidized and reduced forms of the pumping species (2.5 mM $Ru(NH_3)_6^{2+}$ and 2.5 mM $Ru(NH_3)_6^{3+}$) through openings or ports in the glass lid. (For flow visualization experiments, microbeads were also added to the cell and tracked with video microscopy. Speeds were determined with a particle tracking software (World-In-Motion Physics Toolkit software (WIM, www.physicstoolkit.com)).). The 1:1 mixture provides the auxiliary electrode with electroactive species to counteract current at the working electrode(s) and avoid electrode dissolution and bubble formation. A 1.2 μL solution of 9.6 mM PAP_R for control studies (discussed in the Supporting Information) or 8.3 mM PAPP (for enzyme conversion studies) in the pumping solution was then injected with a micropipette into the cell through the drilled hole upstream of the detecting electrode. The hole was strategically placed far enough from the array region that natural diffusion would take significantly more time than redox-MHD driven fluid flow to deliver species to the detector. The location of the injected fluid was also in line with the expected redox-MHD induced flow path.

Immediately after the plug was injected, the pumping and detecting electrodes were turned on in the presence of a magnetic field. A voltage of −0.25 V vs. the quasi-reference electrodes at one set of pumping electrodes causes reduction there and oxidation at the other set of pumping electrodes (the auxiliary electrodes). In the presence of the magnet, this produces a reinforcing flow[19] pattern which causes solution to move in a path between the two sets of electrodes and across the detector, as illustrated in Figure S-1b in Supporting Information. Square wave

voltammetry (SWV) from −0.3 to 0.4 V at a frequency of 25 Hz and amplitude of 50 mV at the detecting electrode allowed quantification of both, pumping species and PAP_R. Waveforms performed at each electrode are shown in Figure S-5 (a and b) in Supporting Information.

Results and Discussion

To determine compatibility of this redox-MHD system for immunoassay applications, experiments were performed that involved detection of PAP_R that was enzymatically generated by AP from its *electroinactive* PAPP substrate in the presence of the redox-pumping species. This represents the signal transduction step in a typical heterogeneous, sandwich-type electrochemical immunoassay, where an enzyme such as AP is conjugated to a secondary antibody bound to the antigen that had been captured by an immobilized primary antibody. The PAP_R signal would then be proportional to the amount of antigen captured.[29]

Selection of the pumping method and of the pumping species for compatibility with PAP_R is described in the Supporting Information. (Figures S-2 and S-3 in the Supporting Information show SWV responses and corresponding calibration curves of PAP_R in the absence and presence of the pumping species, 2.5 mM $Ru(NH_3)_6^{2+}$ and 2.5 mM $Ru(NH_3)_6^{3+}$, respectively. The presence of the pumping species worsens the detection limits for PAP_R by a factor of 4.5 (from 5.69 ± 0.19 μM to 25.5 ± 1.0 μM). Limits of detection are discussed further in the Supporting Information and compared to those in the literature). The electrochemical cell was filled with 2.5 mM $Ru(NH_3)_6^{2+}$ and 2.5 mM $Ru(NH_3)_6^{3+}$ in 0.1 M Tris buffer that also contained AP at a concentration of 0.5 μM, which is more than sufficient for expedient conversion of PAPP to the electrochemically active species, PAP_R.[30] A plug of 8.3 mM PAPP, in the pumping solution, was injected into the cell. Immediately afterwards, the pumping and detecting electrodes were turned on in the presence of a magnetic field. A top-down schematic representation of the movement of the plug from the injection site, across the array region, and to the detector is shown in Figure 1a. A side-view schematic representation of the chemical and electrochemical reactions occurring in the cell is shown in Figure 1b. At the periphery of the plug, AP converts PAPP to PAP_R. At the working set of pumping electrodes, reduction of $Ru(NH_3)_6^{3+}$ takes place, while at the counter set of pumping electrodes, oxidation of $Ru(NH_3)_6^{2+}$ occurs. A steady-state current of ~2.1 μA was achieved at the pumping electrodes. Oxidation via SWV of both $Ru(NH_3)_6^{2+}$ and enzymatically-generated PAP_R takes place at the detecting electrode.

Consecutive SWV responses at the detecting electrode, demonstrating simultaneous monitoring of pumping species and PAP_R over time are shown in Figure 1c. It is observed that PAP_R is enzymatically generated in the plug, pumped across the detector, detected there, and then pumped away from the detector. PAP_R began to be detectable at ~50 s after introduction of the plug. The signal continued to increase until it reached a maximum of 0.48 μA at ~150 s. This current is only 9% of that which would be expected for an 8.3 mM solution of PAP_R (if complete conversion of PAPP to PAP_R were to take place) and corresponds to a concentration of enzymatically-generated PAP_R of 0.65 mM (as determined from the calibration curve in Figure S-3, Supporting Information). The plug will undergo dilution as it travels from the injection port to the detector, which is responsible for some of the current loss, but it is also possible that there is incomplete conversion of PAPP to PAP_R as is further discussed below.

The change of signal with time can be used to quantify the speed with which the plug components reach the detector. Thus, a plot of PAP_R signal over time is given in Figure 1d. The regression line for the delivery of enzymatically-generated PAP_R to the detector when the experiment was run in full operation, that is, pumping and detecting electrodes active in the presence of a magnet was $y = 0.0071\ \mu A/s\ x - 0.31\ \mu A$ ($R^2 = 0.994$). When the pumping

electrodes were left off as a control experiment, the maximum peak current was only 25% that of the maximum peak current from full operation and the best fit line was y = 0.0012 μA/s x - 0.12 μA (R^2 = 0.999), showing a growth of PAP_R signal that was only 17% of that with the pumping electrodes on. In a different control experiment, the absence of a magnetic field revealed an even lower maximum PAP_R peak current at 13% of the full operation maximum current with a best fit line of y = 0.0007 μA/s x - 0.08 μA (R^2 = 0.996), having a slope that is only 9.9% of that in full operation. A final control experiment in which AP was not present in the surrounding solution revealed no enzymatically generated PAP_R and results are overlain in Figure 1d.

These results show that the introduction and removal of in situ-generated PAP_R was most efficient during full operation, where the slope is six to ten times of those from the control experiments. This indicates that the arrival of the plug is not just due to diffusion, but rather due to substantial redox-MHD pumping that takes place, even with the low concentration of pumping species. The presence of the detecting electrode in a magnetic field does contribute to the overall redox-MHD flow, although it is small. Visualization studies with microbeads showed that this contribution took the form of a zig-zag flow pattern between the pumping electrodes (see Figure S-5 in the Supplementary Information). Natural diffusion of PAP_R to the detector also occurs but is much slower than any redox-MHD induced convection.

A series of control experiments were performed like those above, but in which PAP_R replaced PAPP in the injected plug and there was no AP in the surrounding solution. Results in Figures S-4a and S-4b in Supporting Information for detecting PAP_R directly are consistent with those in Figure 1c and 1d for detecting the enzymatically-generated PAP_R, thus confirming the interpretation of the data. However, the maximum current for the detection of enzymatically-generated PAP_R was only 67% of that expected for a plug of PAP_R injected directly into the cell and having the same starting concentration as the PAPP. (See Figure S-4b and discussion of control experiments in Supporting Information.) Because dilution effects should be similar for a plug containing PAPP and a plug containing PAP_R, the lower current for the enzymatically generated PAP_R in the PAPP plug is likely due to insufficient time for complete conversion of the PAPP to PAP_R before the injected plug reached the detector.

Conclusions

It has been demonstrated for the first time that pumping via redox-MHD, from oxidation and reduction of redox species at large microband electrodes, can be used to deliver a different electroactive species to a separate microelectrode for electrochemical detection there, all on a single device. This was accomplished by using a low concentration of a redox-pumping species (5 mM total) so that detection of a separate analyte, in its presence, was possible without having to physically remove the pumping species before detection, thus overcoming original concerns of using redox-MHD for analytical applications. This is the lowest concentration reported to date to induce redox-MHD convection at microelectrodes in the presence of a low B-field for microfluidics in small volumes. A suitable pumping species ($Ru(NH_3)_6^{2+}$ and $Ru(NH_3)_6^{3+}$) for detection of PAP_R, the product of a common enzymatic reaction used in electrochemical immunoassays, while maintaining AP enzyme activity, and compatibility with enzyme substrate and buffer was found. Simultaneous pumping without a channel to guide a fluid plug (via redox-MHD) and detection (via electrochemistry) is possible. Channelless designs provide great flexibility in device fabrication. Directing flow to specific locations at different times is easily accomplished by activating different electrodes patterned on a chip. It was determined that a small detecting electrode between pumping electrodes does not significantly alter flow velocities or trajectories. These preliminary results suggest that integrating redox-MHD microfluidics into a device offers unique opportunities for and is compatible with lab-on-a-chip applications. Future work will involve performing a full, multi-step assay which will

require a modified microfluidic design to perform multi-solution introduction and removal as well as regions for mixing on-chip to decrease incubation times.

Supplementary Material

Refer to Web version on PubMed Central for supplementary material.

Acknowledgments

We acknowledge financial support through a grant from the National Science Foundation (CHE-0719097). The project was also partially supported by Award Number P20RR015569 from the National Center for Research Resources. The content is solely the responsibility of the authors and does not necessarily represent the official views of the National Center for Research Resources or the National Institutes of Health. We thank Errol Porter and Mike Glover at the University of Arkansas High Density Electronics Center for assistance with fabrication. We also thank Caitlin Williams for helpful discussions regarding PAPP synthesis and Anna Daily for assistance in drying synthesized PAPP.

References

(1). Manz A, Graber N, Widmer HM. Sensors and Actuators B-Chemical 1990;1:244–248.

(2). Bruin GJM. Electrophoresis 2000;21:3931–3951. [PubMed: 11192117]

(3). Harrison DJ, Manz A, Fan ZH, Ludi H, Widmer HM. Analytical Chemistry 1992;64:1926–1932.

(4). Whitesides GM, Stroock AD. Physics Today 2001;54:42–48.

(5). Aguilar ZP, Arumugam PU, Fritsch I. Journal of Electroanalytical Chemistry 2006;591:201–209.

(6). Arumugam PU, Fakunle ES, Anderson EC, Evans SR, King KG, Aguilar ZP, Carter CS, Fritsch I. J. Electrochem. Soc 2006;153:E185–E194.

(7). Qian SZ, Bau HH. Mechanics Research Communications 2009;36:10–21. [PubMed: 20046890]

(8). Weston MC, Gerner MD, Fritsch I. Analytical Chemistry 2010;82:3411–3418. [PubMed: 20380431]

(9). Bau HH, Zhu JZ, Qian SZ, Xiang Y. Sensors and Actuators B-Chemical 2003;88:205–216.

(10). Eijkel JCT, Dalton C, Hayden CJ, Burt JPH, Manz A. Sensors and Actuators B 2003;92:215–221.

(11). Homsy A, Linder V, Lucklum F, de Rooij NF. Sensors and Actuators B-Chemical 2007;123:636–646.

(12). Jang J, Lee SS. Sensors and Actuators A 2000;80:84–89.

(13). Nguyen B, Kassegne SK. Microfluidics and Nanofluidics 2008;5:383–393.

(14). West J, Karamata B, Lillis B, Gleeson JP, Alderman J, Collins JK, Lane W, Mathewson A, Berney H. Lab Chip 2002;2:224–230. [PubMed: 15100815]

(15). Zhong JH, Yi MQ, Bau HH. Sensors and Actuators a-Physical 2002;96:59–66.

(16). Anderson EC, Fritsch I. Anal. Chem 2006;78:3745–3751. [PubMed: 16737232]

(17). Clark EA, Fritsch I. Anal. Chem 2004;76:2415–2418. [PubMed: 15080758]

(18). Weston MC, Anderson EC, Arumugam PU, Yoga Narasimhan P, Fritsch I. Analyst 2006;131:1322–1331. [PubMed: 17124540]

(19). Anderson EC, Weston MC, Fritsch I. Analytical Chemistry 2010;82:2643–2651. [PubMed: 20210341]

(20). Bange A, Halsall HB, Heineman WR. Biosensors and Bioelectronics 2005;20:2488–2503. [PubMed: 15854821]

(21). Duan CM, Meyerhoff ME. Analytical Chemistry 1994;66:1369–1377. [PubMed: 8017631]

(22). Fakunle ES, Aguilar ZP, Shultz JL, Toland AD, Fritsch I. Langmuir 2006;22:10844–10853. [PubMed: 17129069]

(23). Aguilar ZP, Vandaveer WR, Fritsch I. Analytical Chemistry 2002;74:3321–3329. [PubMed: 12139035]

(24). Driskell JD, Uhlenkamp JM, Lipert RJ, Porter MD. Analytical Chemistry 2007;79:4141–4148. [PubMed: 17487976]

(25). Choi JW, Oh KW, Thomas JH, Heineman WR, Halsall HB, Nevin JH, Helmicki AJ, Henderson HT, Ahn CH. Lab on a Chip 2002;2:27–30. [PubMed: 15100857]

(26). Niwa O, Xu Y, Halsall HB, Heineman WR. Analytical Chemistry 1993;65:1559–1563. [PubMed: 8328672]

(27). Thompson RQ, Porter M, Stuver C, Halsall HB, Heineman WR, Buckley E, Smyth MR. Analytica Chimica Acta 1993;271:223–229.

(28). Deriemer LH, Meares CF. Biochemistry 1981;20:1606–1612. [PubMed: 6164387]

(29). Tang HT, Lunte CE, Halsall HB, Heineman WR. Analytica Chimica Acta 1988;214:187–195.

(30). Kreuzer MP, O'Sullivan CK, Guilbault GG. Analytica Chimica Acta 1999;393:95–102.

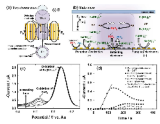

Figure 1.

(a) Top-down representation of pumping a plug (purple circle) at three different times from the injection site (at bottom of diagram) to the detecting electrode (at top) via reinforcing flow between pumping electrodes. (b) Side-view of the electrochemical cell showing enzymatic conversion of PAPP to PAP_R via AP at the periphery of the plug (purple) and electrochemical determination of PAP_R at the detecting electrode ($PAP_R \rightarrow PAP_O + 2\,H^+ + 2\,e^-$). The oxidation and reduction of $Ru(NH_3)_6^{2+}$ and $Ru(NH)_3)_6^{3+}$, respectively,

($Ru(NH_3)_6^{2+} \underset{\leftarrow}{\rightarrow} Ru(NH_3)_6^{3+} + 1e^-$) at pumping electrodes in the presence of a magnetic field move the plug. The direction of the ion flux, magnetic flux density, and resulting $\mathbf{F_B}$ (flow) are indicated. (c) SWV responses showing delivery of enzymatically-generated PAP_R to the detecting electrode with redox-MHD pumping over time. (d) Plots of SWV peak current of enzymatically generated PAP_R as a function of time show arrival and removal of enzymatically-generated PAP_R. Filled circles show results when active pumping and detecting electrodes were on in the presence of a magnetic field (full operation). Filled squares are for a control study when pumping electrodes were off, but the detector was on in the presence of the magnetic field. Open circles correspond to an experiment when pumping and detecting electrodes were on, but in the absence of a magnetic field. Stars represent results when AP was not present in the surrounding solution, but otherwise the device was in full operation. The solid line is the regression curve used to calculate the slope for the plug arrival rate involving the full operation. Regression curves were determined for the control experiments, too, but are not shown in this figure.